www.ietdl.org

Published in IET Microwaves, Antennas & Propagation
Received on 29th August 2013
Revised on 3rd May 2014
Accepted on 3rd July 2014
doi: 10.1049/iet-map.2013.0473

ISSN 1751-8725

Evaluating radiation efficiency from characteristic currents

Miloslav Capek, Jan Eichler, Pavel Hazdra

Department of Electromagnetic Field, Faculty of Electrical Engineering, Czech Technical University in Prague, Technicka 2, 16627, Prague, Czech Republic
E-mail: miloslav.capek@fel.cvut.cz

Abstract: This study describes an effective technique for calculating modal radiation efficiency calculation based on decomposition into characteristic modes. The key assumption is that the current distribution on the perfect electric conductor is almost the same as in the case of a very good conductor, for example, metals such as copper, aluminium and silver. This assumption is verified against the conventional technique, the impedance boundary condition (IBC). The proposed approach does not require any modification of the formulation of method of moments for perfectly conducting surfaces, which is assumed for the modal decomposition. Modal efficiencies provide an additional insight that is useful especially for the design of small antennas. Taking the feeding into account, the modal losses can be summed up to obtain the total efficiency. The technique works perfectly for common metals, is fully comparable with the IBC, and can easily be incorporated into any present-day in-house solver. A numerical analysis of three antennas is presented to demonstrate the merits of the approach. Radiation efficiency of coupled dipoles, an electrically small meandered dipole, and PIFA were investigated by the presented method. The results are in perfect agreement with the reference commercial package.

1 Introduction

Antenna radiation efficiency [1] is a very important parameter, especially if the electrical dimensions are small [2]. A common approach for computing the radiation efficiency of an antenna is to take a lossy material into account in the numerical simulation. This approach is general and accurate, but it does not provide much physical insight into the lossy antenna operation.

In the proposed approach, the current density evaluated on a perfect electric conductor (PEC) is assumed to be approximately the same as for a lossy metal of infinite thickness. It will be shown that this assumption works perfectly for common metals such as copper and aluminium. Moreover, the radiation efficiency can be evaluated very quickly in a post-processing step, once the currents on PEC are evaluated by the method of moments (MoM) solver.

A more precise evaluation is based on the surface impedance boundary condition (IBC) [3, 4]. However, time-consuming recalculation of the MoM matrix is needed whenever the conductivity σ or the thickness t of the metal is changed.

To gain a better physical picture of the operation of a lossy antenna, the theory of characteristic modes (TCM) [5–7] is adopted for calculating individual modal efficiencies. This theory enables to calculate a set of so-called characteristic currents by decomposition of the MoM impedance matrix. These currents are orthogonal (with respect to the radiated power), and may be summed to form the total current flowing on an antenna if the feeding is connected. Thus TCM makes it possible to study the antenna geometry without the specific feeding, and to understand its operation through modal superposition of various quantities based on the surface current density [8, 9]. Remark that very simple calculation of the (modal) radiation efficiency has already been treated in [10] where the skin effect was not taken into account and no summation of the modal losses was presented.

This paper develops a fast and physically illustrative procedure for approximating the radiation losses for characteristic modes particularly on RWG [11] meshes, but the technique is not limited to any discretisation scheme.

2 Calculating the radiation efficiency from surface currents

Expressions for calculating the radiation efficiency will be derived in this section. The input of the procedure is an antenna consisting of an infinitesimally thin PEC. Next, suppose that the antenna is discretised using the RWG basis functions and the current density is computed by the MoM [12].

Begin with the definition of the radiation efficiency [1]

$$\eta = \frac{P^{\mathrm{R}}}{P^{\mathrm{R}} + P^{\mathrm{L}}} \qquad (1)$$

where P^{R} is the radiated power and P^{L} is the power loss. If no losses are present (i.e. a PEC antenna in a lossless dielectric), P^{R} is equal to the power received by the antenna from the feed port. It is therefore needed to compute P^{L} if there were losses in the metal. The procedure is as follows.

Suppose a PEC surface on which the surface current density $\boldsymbol{J}^{\text{surf}}$ is computed by the MoM. Next, the skin-effect will be taken into account by introducing the equivalent volume current density

$$\boldsymbol{J}^{\text{eq}}(z) = \boldsymbol{J}_0^{\text{eq}}\, \mathrm{e}^{-(1+j)\gamma z} \tag{2}$$

where z is the distance from the metal surface, and the attenuation constant [13] for a highly conductive material is

$$\gamma = \sqrt{\frac{\omega\mu\sigma}{2}} \tag{3}$$

where μ is the permeability and ω is the angular frequency. Now, it is assumed that the current flowing on the perfectly conducting body has the same shape as if small losses are introduced

$$\left|\int_0^t \boldsymbol{J}^{\text{eq}}(z)\mathrm{d}z\right| = \left|\boldsymbol{J}^{\text{surf}}\right| \tag{4}$$

and also that the metallisation thickness t is high enough to neglect the reflection from the other side of the metal body. From (2) and (4) one obtains

$$\left|\boldsymbol{J}_0^{\text{eq}}\right| = \frac{\sqrt{2}\gamma\left|\boldsymbol{J}^{\text{surf}}\right|}{\left|1 - \mathrm{e}^{-(1+j)\gamma t}\right|} \tag{5}$$

Considering now a triangulated surface and constant current $\boldsymbol{J}_n^{\text{surf}}$ on each triangle n, the power loss can be expressed as [13]

$$\begin{aligned} P^{\mathrm{L}} &= \int_{\Omega} \boldsymbol{E}\cdot\boldsymbol{J}^{*}\mathrm{d}V \simeq \sum_n \int_{\Omega} \frac{\left|\boldsymbol{J}_n^{\text{eq}}\right|^2}{\sigma}\mathrm{d}V \\ &= F(\omega,\sigma,t)\sum_n A_n\left|\boldsymbol{J}_n^{\text{surf}}\right|^2 \end{aligned} \tag{6}$$

where * denotes the complex conjugation, A_n is the area of triangle n, $\Omega = \bigcup_n A_n$ is the PEC surface, and

$$F(\omega,\sigma,t) = \frac{\gamma}{\sigma}\frac{(1 - \mathrm{e}^{-2\gamma t})}{\left|1 - \mathrm{e}^{-(1+j)\gamma t}\right|^2} \tag{7}$$

3 Modal radiation efficiency

The radiation efficiency of a certain characteristic current will be defined in this section. Then a summation formula for these modal radiation efficiencies is obtained. The physical background of how particular modes contribute to the overall radiation efficiency can be thus explored. Since it is enough to include only the first few modes [14] for an electrically small antenna, this knowledge can help the designer to modify the antenna geometry to suppress certain modes and increase the overall radiation efficiency of the antenna. The second goal is to derive a fast formula for computing and optimising the radiation efficiency. Recall that for a certain structure at a given frequency, the impedance matrix does not need to be recalculated and the total radiation efficiency is controlled only through the position of the feeding port that affects the expanding coefficients.

3.1 Theory of characteristic modes

The principles of the TCM which are important for defining the modal radiation efficiency are briefly presented here. A detailed description of TCM and its derivation can be found in [5] and a recent revision in [7].

The theory is based on eigen-decomposition of the electric field integral equation operator [15] $\mathcal{Z}(\boldsymbol{J}) = \mathcal{R}(\boldsymbol{J}) + j\mathcal{X}(\boldsymbol{J})$ on a PEC surface, according to the generalised eigenvalue problem

$$\mathcal{X}\boldsymbol{J}_u = \lambda_u \mathcal{R}\boldsymbol{J}_u \tag{8}$$

where λ_u is the uth characteristic number (eigenvalue) and $\boldsymbol{J}_u$ is the characteristic vector or current [5]. All modal current densities are normalised [5] at every frequency to radiate the power $P_u^{\mathrm{R}} = 1\mathrm{W}$

$$\langle \boldsymbol{J}_u, \mathcal{R}\boldsymbol{J}_u\rangle = 1 = P_u^{\mathrm{R}} \tag{9}$$

where the symmetrical product was used. Note here, that the symmetrical product of $\boldsymbol{a}$, $\boldsymbol{b}$ is defined as $\langle \boldsymbol{a}, \boldsymbol{b}\rangle = \int_{\Omega} \boldsymbol{a}\cdot\boldsymbol{b}\,\mathrm{d}\Omega$, and the dot product is defined in the usual way as $\boldsymbol{a}\cdot\boldsymbol{b} = \sum a_i b_i$ was used. Thus the modes satisfy the orthogonality relations

$$\langle \boldsymbol{J}_u, \mathcal{R}\boldsymbol{J}_v\rangle = \delta_{uv} \tag{10}$$

$$\langle \boldsymbol{J}_u, \mathcal{X}\boldsymbol{J}_v\rangle = \lambda_u\delta_{uv} \tag{11}$$

$$\langle \boldsymbol{J}_u, \mathcal{Z}\boldsymbol{J}_v\rangle = (1 + \lambda_u)\delta_{uv} \tag{12}$$

where δ_{uv} is the Kronecker delta function, [3] $\delta_{uv} = 0$ for $u \neq v$ and $\delta_{uv} = 1$ for $u = v$. The total current on the antenna surface can be found by summation as [5]

$$\boldsymbol{J} = \sum_u \alpha_u \boldsymbol{J}_u \tag{13}$$

For an impressed field $\boldsymbol{E}^{\mathrm{i}}$, representing the excitation, the expanding coefficients α_u are [5]

$$\alpha_u = \frac{\langle \boldsymbol{J}_u, \boldsymbol{E}^{\mathrm{i}}\rangle}{1 + j\lambda_u} \tag{14}$$

3.2 Deriving the modal radiation efficiency

Considering surface current density $\boldsymbol{J}^{\text{surf}}$ expressed as a superposition of the characteristic modes according to (13), $\left|\boldsymbol{J}_n^{\text{surf}}\right|^2$ reads

$$\begin{aligned} \left|\boldsymbol{J}_n^{\text{surf}}\right|^2 &= \sum_u \alpha_u \boldsymbol{J}_{nu}^{\text{surf}} \cdot \sum_v \alpha_v^{*}(\boldsymbol{J}_{nv}^{\text{surf}})^{*} \\ &= \sum_u\sum_v \beta_{uv}\boldsymbol{J}_{nu}^{\text{surf}}\cdot(\boldsymbol{J}_{nv}^{\text{surf}})^{*} \end{aligned} \tag{15}$$

The coupling $\boldsymbol{\beta} = [\beta_{uv}]$ matrix is defined in [8] as

$$\beta_{uv} = \Re\{\alpha_u\alpha_v^{*}\} = \frac{\langle \boldsymbol{J}_u, \boldsymbol{E}^i\rangle\langle \boldsymbol{J}_v, \boldsymbol{E}^i\rangle(1 + \lambda_u\lambda_v)}{(1 + \lambda_u^2)(1 + \lambda_v^2)} \tag{16}$$

The modal power loss is

$$P_{uv}^{\mathrm{L}} = F(\omega, \sigma, t) \sum_{n} A_n \boldsymbol{J}_{nu}^{\mathrm{surf}} \cdot \boldsymbol{J}_{nv}^{\mathrm{surf}} \tag{17}$$

Note that the characteristic currents are real by definition [5], so the complex conjugation rising from (15) can be omitted. Since the modal radiated power is normalised to 1 W, the modal radiation efficiency of mode u is expressed as

$$\eta_u = \frac{1}{1 + P_{uu}^{\mathrm{L}}} \tag{18}$$

The total power loss may now be expressed as a superposition of the modal radiation losses

$$P^{\mathrm{L}} = \sum_u \sum_v \beta_{uv} P_{uv}^{\mathrm{L}} = \langle \boldsymbol{\beta}, \boldsymbol{P}^{\mathrm{L}} \rangle \tag{19}$$

Using the orthogonal property of characteristic modes (9) and (1), the radiation efficiency is finally written as

$$\eta = \frac{\sum_u \beta_{uu}}{\sum_u \beta_{uu} + \sum_u \sum_v \beta_{uv} P_{uv}^{\mathrm{L}}} = \frac{\mathrm{Tr}(\boldsymbol{\beta})}{\mathrm{Tr}(\boldsymbol{\beta}) + \langle \boldsymbol{\beta}, \boldsymbol{P}^{\mathrm{L}} \rangle} \tag{20}$$

4 Numerical results

To verify the presented derivation is valid and that the approximations that have been made are reasonable, three test structures were chosen. The test structures are a meandered strip dipole (Fig. 1), a coupled active and parasitic dipole (Fig. 2) and a PIFA antenna [16] over a finite ground plane (Fig. 3). Note that these cases were computed in a wide frequency range and are of various types (electrically small, planar, strips, highly resonant structures, with and without a finite ground plane).

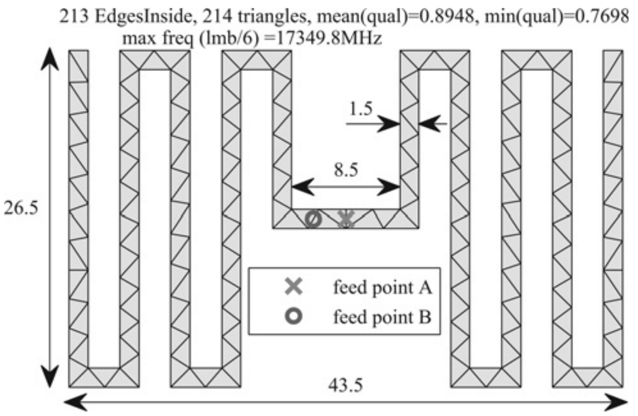

Fig. 1 *Triangular mesh of the meandered dipole with various feeding points, dimensions are in (mm)*

The 'qual' means the quality of triangles ('mean' is the average quality and 'min' is the quality of the worst triangle), and 'max freq' (lmb/6) is related to the highest frequency that can be safely calculated under the condition that the edges length is <λ/6

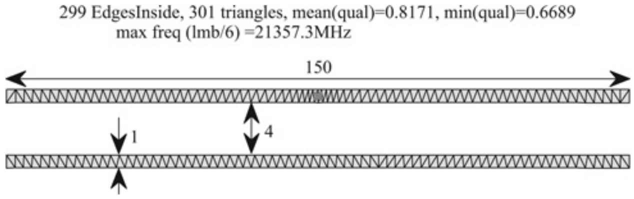

Fig. 2 *Triangular mesh of coupled dipoles. Feeding point is at the top dipole, marked by the green cross. Dimensions are in (mm)*

The 'qual' means the quality of triangles ('mean' is the average quality and 'min' is the quality of the worst triangle), and 'max freq' (lmb/6) is related to the highest frequency that can be safely calculated under the condition that the edges length is <λ/6

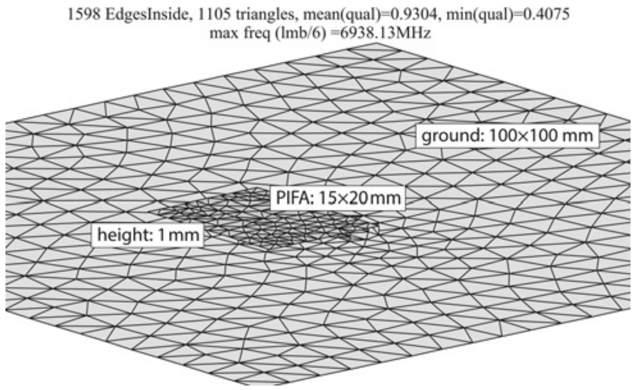

Fig. 3 *Detailed view of the triangular mesh of the PIFA*

The 'qual' means the quality of triangles ('mean' is the average quality and 'min' is the quality of the worst triangle), and 'max freq' (lmb/6) is related to the highest frequency that can be safely calculated under the condition that the edges length is <λ/6

4.1 Effect of changes in current distribution between the lossy case and the lossless case

In Section 2, it has been assumed that the current distribution on an antenna made of thin metal (with $\sigma > 10^5$ S/m) and on an antenna made of PEC is approximately the same. The validity of this important assumption will be numerically verified in this section.

The centre-fed meandered dipole, Fig. 1, feed point A, was modelled in FEKO [17] and the current density as well as the area of the triangular elements was exported in ASCII format. The data for $\sigma = \{5.85 \times 10^7, 5.85 \times 10^6, 5.85 \times 10^5\}$ S/m and for PEC were imported into the Matlab [18] routine, and the total radiation efficiency was computed according to (6) and (1), see Fig. 4 for a comparison.

The differences between the radiation efficiency computed from the currents on a PEC antenna and on a lossy antenna are generally very small. The same procedure was repeated for each of the test structures and for all combinations of $\sigma = \{5.85 \times 10^7, 5.85 \times 10^6, 5.85 \times 10^5\}$ S/m and $t = \{18, 50\}$ μm, that is, 18 different cases. The results were qualitatively similar to Fig. 4. It should be mentioned that the radiation efficiency minimum computed from the PEC currents was slightly shifted upwards in frequency (25 MHz shift at 8 GHz for a meandered dipole, $\sigma = 5.85 \times 10^5$ S/m, $t = 50$ μm), Fig. 4. However, this 0.3 % frequency shift for low-conductivity metals can be neglected for practical purposes. Thus it is concluded that the assumptions of Section 2 hold very well for all tested combinations.

IET Microw. Antennas Propag., 2015, Vol. 9, Iss. 1, pp. 10–15
doi: 10.1049/iet-map.2013.0473

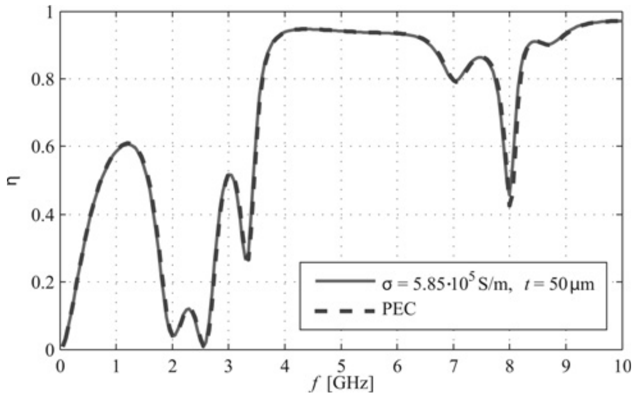

Fig. 4 *Computation of radiation efficiency from currents on PEC and a lossy surface*

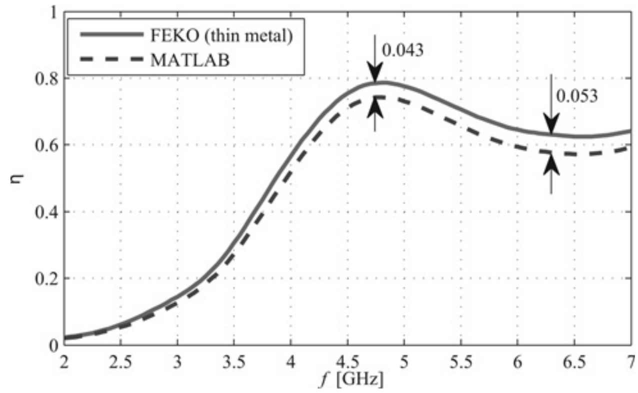

Fig. 7 *Radiation efficiency computed by FEKO and by MATLAB*
PIFA, $\sigma = 5.85 \times 10^5$ S/m, $t = 50$ μm

4.2 MoM solution using an in-house software tool

In this section, the results using a commercial software package will be compared with the in-house MoM tool [9]. The tool is based on [19], and only considers perfectly conducting metal bodies. The power loss is computed according to (6). In FEKO, the structure is modelled as infinitesimally thin, but t and σ are defined for a material model based on the IBC [20] that is used in the simulation. Figs. 5–7 show that these two approaches give very similar results. The biggest difference for PIFA and low σ is plotted in Fig. 7. Thus it is seen that FEKO (MoM + IBC) and MATLAB code (MoM on PEC + (6)) give very comparable results.

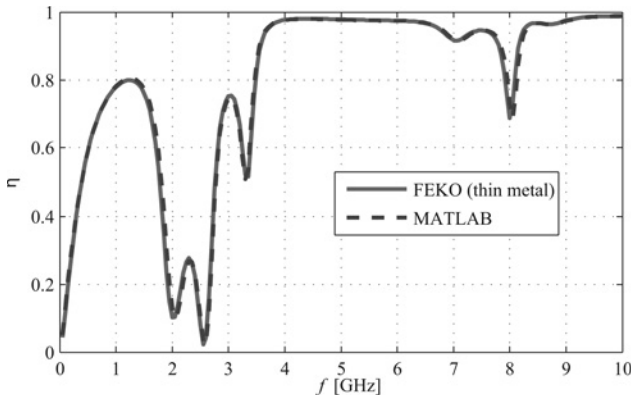

Fig. 5 *Radiation efficiency computed by FEKO and by MATLAB*
Meandered dipole, $\sigma = 5.85 \times 10^6$ S/m, $t = 50$ μm

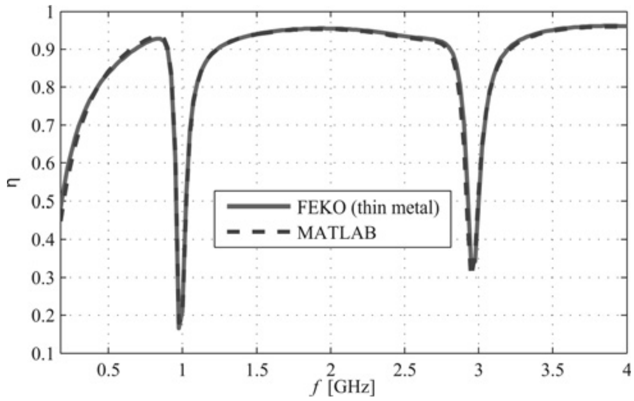

Fig. 6 *Radiation efficiency computed by FEKO and by MATLAB*
Coupled dipoles, $\sigma = 5.85 \times 10^6$ S/m, $t = 18$ μm

4.3 Modal radiation efficiency

Features of modal radiation efficiency will be demonstrated using the example of a meandered dipole discussed in the previous section. The impedance matrix obtained by the in-house MoM tool is decomposed into characteristic modes [9]. The beta matrix (16) and the modal power loss matrix (17) are computed from this set of modes. Using these inputs, the total radiation efficiency η is computed using (20), and is compared with the MoM solution. The structure was approximated by 213 basis functions, and all 213 numerically computed modes were used in the superposition. The two results are almost equivalent (see Fig. 8), which is in correspondence with the theoretical development of Section 3.2. The small difference can be ascribed to numerical errors arising from computationally difficult decomposition.

The contribution of modal losses to the total radiation efficiency will be now investigated by studying the effect of the asymmetrical feeding point of the meandered dipole in Fig. 1 (position 'B'). It is clearly seen that a new minimum of radiation efficiency is present at 1.6 GHz, as shown in Fig. 9.

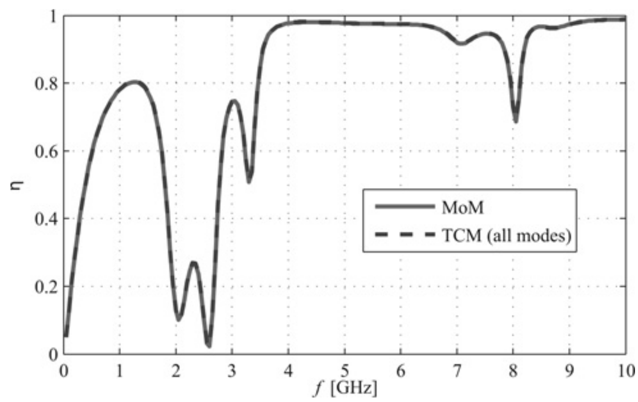

Fig. 8 *Radiation efficiency computed from the MoM result and through modal superposition*
Meandered dipole, $\sigma = 5.85 \times 10^6$ S/m, $t = 50$ μm

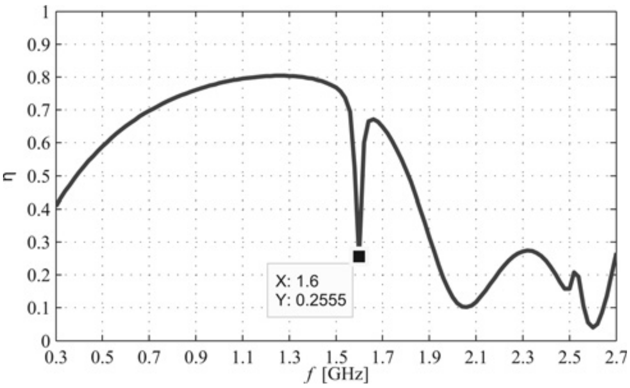

Fig. 9 *Radiation efficiency of the asymmetrically fed (feed point B)*
Meandered dipole, σ = 5.85 × 10^6 S/m, t = 50 μm

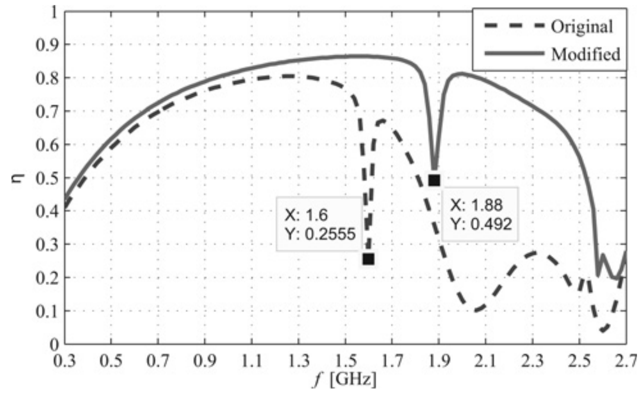

Fig. 12 *Comparison of the radiation efficiency of the modified and the original meandered dipole, feed point B, σ = 5.85 × 10^6 S/m, t = 50 μm*

Table 1 Diagonal terms of the coupling matrix, the modal power loss matrix and the modal radiation efficiency at 1.6 GHz

U	β_{uu}	P^{L}_{uu}	η_{uu}	$\beta_{uu}P^{L}_{uu}$
1	8.62×10^{5}	0.084	**0.92**	7.25×10^{6}
2	2.03×10^{4}	2.25	**0.31**	4.56×10^{4}
3	2.36×10^{7}	0.05	0.95	1.19×10^{8}
4	1.71×10^{6}	1.16	0.46	1.98×10^{6}
5	1.65×10^{7}	1.83	0.35	3.00×10^{7}
6	8.75×10^{11}	5.85	0.15	5.12×10^{10}
7	1.60×10^{8}	61.96	0.016	9.91×10^{7}

The modal efficiencies of the significant modes are bold

The structure was decomposed into characteristic modes; see β_{uu} and P^{L}_{uu} in Table 1 for the first seven modes. Although the cross terms, that is, the β_{uv}, P^{L}_{uv}; $u \neq v$ are necessary in (20), the main information about the significance in the sum of radiation efficiencies is readable from the diagonal terms only. From Table 1, it is evident that the dominantly excited modes are modes 2 and 1. While mode 1 is desired and radiates well, mode 2 has low modal radiation efficiency ($\eta_{22} = 31\%$) and thus it contributes strongly to power loss.

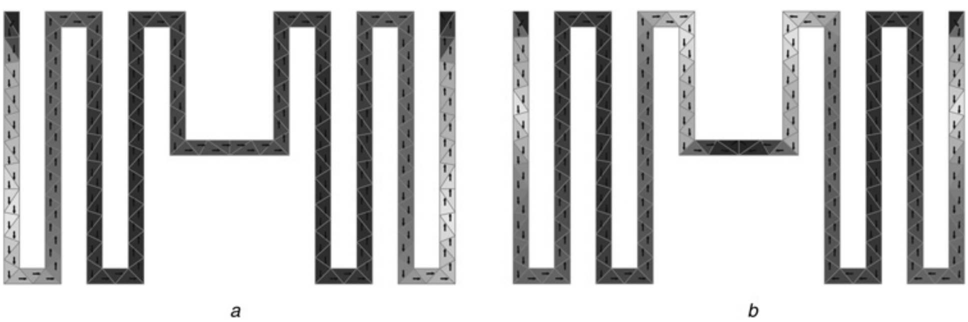

Fig. 10 *Characteristic current at 1.6 GHz*
a Mode 1
b Mode 2

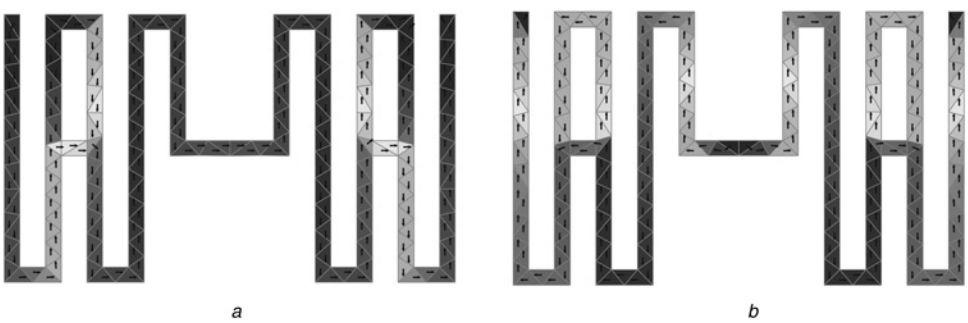

Fig. 11 *Modified meandered dipole, characteristic current, 1.88 GHz*
a Mode 1
b Mode 2

doi: 10.1049/iet-map.2013.0473

Table 2 Diagonal terms of the coupling matrix, modal power loss matrix and modal radiation efficiency of the modified meander at 1.88 GHz

u	β_{uu}	P^{L}_{uu}	η_{uu}	$\beta_{uu}P^{\mathrm{L}}_{uu}$
1	1.25×10^4	0.068	**0.94**	8.57×10^6
2	1.06×10^3	0.51	**0.66**	5.44×10^4
3	1.22×10^9	793	0.0013	9.64×10^7
4	4.20×10^6	0.073	0.93	3.08×10^7
5	2.63×10^6	0.84	0.54	2.22×10^6
6	3.12×10^9	0.85	0.54	2.67×10^9
7	1.66×10^6	2.85	0.26	4.75×10^6

The modal efficiencies of the significant modes are bold

Next, it would be useful to eliminate the efficiency drop at 1.6 GHz. This is a difficult task from the design point of view, since it is not clear how to achieve this goal from the MoM solution. However, TCM gives guidance that mode 2 should be suppressed or shifted in frequency. Thus the meander should be modified to affect mode 2, while not affecting mode 1; see Fig. 10. A good position for the modification is in the area where the currents of mode 2 are at their maximum, that is, approx. at the centre of the meander arm. The modes on a modified structure are shown in Fig. 11.

The positive effect of the modification on η can be seen in Fig. 12. The current path for mode 2 is shortened, which shifts its resonant frequency from 1.6 to 1.88 GHz. The resonance of mode 1 is also slightly shifted from 0.96 to 1.02 GHz (computed by TCM). Since the current of mode 2 on the modified structure flows less in the opposing directions, η_{22} rises from 31 to 66%, see Table 2. This is reflected in the η in Fig. 12, where the efficiency drop is not as deep as for the original meander.

Another interesting fact is that $\eta = 49.2\%$ at 1.88 GHz, whereas the modal $\eta_2 = 66.12\%$. One would achieve $\eta = \eta_2$ if only mode 2 was excited. However, non-zero contributions to P^{L} from all modes are shown in Table 2. Thus in practice, the η at the resonant frequency of a certain mode u is always lower than the corresponding η_u.

5 Conclusions

The theory for evaluating radiation efficiency from characteristic currents has been presented. It has been shown that the conduction loss (and thus the radiation efficiency) can be understood as the weighted sum of the losses associated with the characteristic modes. The assumptions made in the derivation hold very well for the test structures, namely a meandered dipole, coupled dipoles and PIFA over a finite ground plane and several different metalisation thicknesses and conductivities.

The main advantage of the proposed technique lies in the physical interpretation of the sources of conduction losses which contribute to the overall radiation efficiency. This has been demonstrated on a simple example of an asymmetrically fed meandered dipole, which was modified to improve the radiation efficiency. Another benefit of the technique is the easy implementation to any MoM code. The radiation efficiency computation can be performed as a post processing step, which is particularly useful for TCM. This method can also be used in a very fast optimisation loop.

It is assumed that the extension to the dielectrics bodies is possible following a similar approach. This is a subject of further research, where the formulation of volumetric currents in the dielectrics is utilised.

6 Acknowledgments

The authors would like to thank Dr. M. Polivka for the initial tests in the IE3D software, and Professor J. Vrba and Mr. P. Hamouz for their comments. Also, we would like to thank two anonymous reviewers who suggested valuable improvements to the paper. This work was supported by the Project P102/12/2223 of the Czech Science Foundation, and by the Project SGS14/190/OHK3/3 T/13 of the Grant Agency of the Czech Technical University in Prague.

7 References

1 Balanis, C.A.: 'Antenna theory analysis and design' (Wiley, 2005, 3rd edn.)
2 Volakis, J.L., Chen, C., Fujimoto, K.: 'Small antennas: miniaturization techniques and applications' (McGraw-Hill, 2010)
3 Qian, Z.G., Chew, W.C., Suaya, R.: 'Generalized impedance boundary condition for conductor modeling in surface integral equation', *IEEE Trans. Microw. Theory Tech.*, 2007, **55**, (11), pp. 2354–2364
4 Karlsson, A.: 'Approximate boundary conditions for thin structures', *IEEE Trans. Antennas Propag.*, 2009, **57**, (1), pp. 144–148
5 Harrington, R.F., Mautz, J.R.: 'Theory of characteristic modes for conducting bodies', *IEEE Trans. Antennas Propag.*, 1971, **19**, (5), pp. 622–628
6 Cabedo-Fabres, M.: 'Systematic design of antennas using the theory of characteristic modes', Ph.D. dissertation, UPV, February 2007
7 Cabedo-Fabres, M., Antonino-Daviu, E., Valero-Nogueira, A., Bataller, M.F.: 'The theory of characteristic modes revisited: a contribution to the design of antennas for modern applications', *IEEE Antennas Propag. Mag.*, 2007, **49**, (5), pp. 52–68
8 Capek, M., Hazdra, P., Eichler, J.: 'A method for the evaluation of radiation Q based on modal approach', *IEEE Trans. Antennas Propag.*, 2012, **60**, (10), pp. 4556–4567
9 Capek, M., Hamouz, P., Hazdra, P., Eichler, J.: 'Implementation of the theory of characteristic modes in Matlab', *IEEE Antennas Propag. Mag.*, 2013, **55**, (2), pp. 176–189
10 Hamouz, P., Hazdra, P., Polivka, M., Capek, M., Mazanek, M.: 'Radiation efficiency and Q factor study of franklin antenna using the theory of characteristic modes'. Proc. Fifth European Conf. on Antennas and Propagation (EUCAP), Rome, Italy, April 2011, pp. 1974–1977
11 Rao, S.M., Wilton, D.R., Glisson, A.W.: 'Electromagnetic scattering by surfaces of arbitrary shape', *IEEE Trans. Antennas Propag.*, 1982, **30**, (3), pp. 409–418
12 Gibson, W.C.: 'The method of moments in electromagnetics' (Chapman and Hall/CRC, 2007, 1st edn.)
13 Harrington, R.F.: 'Time-harmonic electromagnetic fields' (IEEE Press, Wiley, 2001, 2nd edn.)
14 Safin, E., Martens, R., Manteuffel, D.: 'Modal source reconstruction based on radiated far-field for antenna design'. Proc. Sixth European Conf. on Antennas and Propagation (EuCAP), 2012, pp. 1645–1649
15 Harrington, R.F.: 'Field computation by moment methods' (IEEE Press, Wiley, 1993)
16 Rowell, C., Lam, E.Y.: 'Mobile-phone antenna design', *IEEE Antennas Propag. Mag.*, 2012, **54**, (4), pp. 14–34
17 EM Software & Systems-S.A. FEKO. Available at: www.feko.info
18 The MathWorks. The Matlab. Available at: www.mathworks.com
19 Makarov, S.N.: 'Antenna and EM modeling with Matlab' (Wiley, 2002)
20 (2013, February) Feko, user's Manual, suite 6.2.2. EM Software & Systems-S.A. (Pty) Ltd. 32 Techno Avenue, Technopark, Stellenbosch, 7600, South Africa. Available at: www.feko.info